ENERGY DISTRIBUTION AND WORK FUNCTION MEASUREMENTS FOR METAL PHOTOCATHODES WITH MEASURED LEVELS OF SURFACE ROUGHNESS

L.B. Jones[1*], T.S. Beaver[2], S. Mistry[3], B.L. Militsyn[1], T.C.Q. Noakes[1], R. Valizadeh[1],
ASTeC[†], STFC Daresbury Laboratory, Warrington, WA4 4AD, United Kingdom
[1] also at The Cockcroft Institute, Warrington, WA4 4AD, United Kingdom
[2] also at Department of Chemistry, Universty of Leicester, LE1 7RH, United Kingdom
[3] also at Department of Physics, University of Loughborough, LE11 3TU, United Kingdom

Abstract

The minimum achievable emittance in an electron accelerator depends strongly on the intrinsic emittance of the photocathode electron source which is measurable as the mean longitudinal and transverse energy spreads in the photoemitted electrons. Reducing emittance in an accelerator driving a Free Electron Laser (FEL) delivers significant reduction in the saturation length for an x–ray FEL, reducing machine cost and increasing x–ray beam brightness.

There are many parameters which affect the intrinsic emittance of a photocathode. Surface roughness is a significant factor, and consequently the development of techniques to manufacture low roughness photocathodes with optimum emission properties is a priority for the electron source community. In this work, we present transverse energy distribution and work function measurements for electrons emitted from copper and molybdenum photocathodes with differing levels of measured surface roughness.

INTRODUCTION

The intrinsic emittance of a photocathode source defines the lowest achievable limit of emittance in a well–configured linear accelerator, and in the absence of space charge, the source emittance can be preserved throughout acceleration in machines of this class [1]. The impact of reducing intrinsic emittance is therefore significant, and can potentially reduce both the physical size and capital cost of a Free-Electron Laser (FEL) facility driven by such an accelerator [2] while also increasing the X–ray beam brightness and hence the machine performance. There are many components which contribute to the overall intrinsic emittance of a photocathode such as composition, crystal face, surface roughness, cleanliness, work function and quantum efficiency (QE), and a change in one of these components can affect both the values of other components and the observed intrinsic emittance for any photocathode.

The issue of surface roughness is of particular interest to the photocathode community. It affects both the local electric field on a microscopic scale and hence the surface voltage which impacts on the accelerating field experienced by photoelectrons [3], and also the Schottky voltage which changes the effective work function [4] and hence the quantum efficiency [5]. Surface roughness also affects the emission geometry which couples directly into mean transverse energy thereby driving emittance growth [6]. Li neatly categorises these effects into either emittance growth due to emission angle or '*slope effect*', and emittance growth due to the induced transverse electric field or '*field effect*' [4].

ASTeC's[†] Transverse Energy Spread Spectrometer (TESS) experimental facility is connected to a Photocathode Preparation Facility (PPF) and can be used with III–V semiconductor, multi–alkali and metal photocathodes to measure transverse and longitudinal energy distributions [7]. Our R&D facilities also include XPS and AFM/STM on our SAPI (Surface Analysis, Preparation and Installation) system [8], with ex–situ interferometric optical and AFM microscopes for roughness measurements. We have carried–out transverse energy spread measurements at a range of illumination wavelengths for copper and molybdenum photocathodes with known levels of surface roughness.

EXPERIMENTAL DETAILS

Samples and Preparation

Experiments were performed on three different 6 mm diameter polycrystalline photocathode samples: one copper with an engineered finish, designated Cu.EF; one copper with a diamond–turned finish, designated Cu.DT; and one molybdenum, designated Mo.

The Cu.EF photocathode was degreased in an acetone bath for 10 minutes, then Ar plasma treated in an ex–situ Henniker Plasma HPT–200 for 20 minutes at 200 W. The photocathode was immediately transferred into our SAPI system and heat cleaned at 450 °C for 1 hour. XPS verified that the sample was atomically–clean. The photocathode was then transferred to the PPF via a vacuum suitcase and heat cleaned at 450 °C for 1 hour.

The Cu.DT and Mo photocathodes were both degreased in acetone for 10 minutes, Ar plasma treated for 20 minutes, then loaded directly into the PPF and heat cleaned at 450 °C for 1 hour. Previous work with our SAPI chamber using XPS has shown that such a cleaning regime leaves an atomically–clean surface for all of these photocathode samples.

* lee.jones@stfc.ac.uk
† ASTeC: Accelerator Science and Technology Centre

ISBN 978-3-95450-182-3

Energy Spread Measurement

Our Xe broadband light source originally configured for GaAs measurements [9] has been optimised for UV performance. The light source, monochromator and optical elements have been installed on a single breadboard, thereby removing the fibre optic link between the monochromator and the beam delivery optics. This increased the UV intensity allowing metal photocathode emission spectra to be recorded. The monochromator exit slit width was 0.6 mm, yielding a spectral bandwidth of (3.0 – 4.0) nm FWHM. The effects of the monochromator slit width influencing spectral bandwidth have been documented previously [9]. A variable iris aperture replaces the fibre optic output coupler as the beam source which is relay–imaged onto the photocathode. A PCO.Ultraviolet beam profile camera [10], whose CCD array was located at the same distance to the photocathode, was used to ensure optimal beam focussing at all wavelengths investigated. The typical beam size was 110 μm FWHM.

An accelerating voltage (U_{acc}) between the photocathode source and detector separated by a drift distance (d) controls the electron flight time (τ). The size of the photoemission footprint (σ) is dependent on the mean transverse energy (MTE) of the photoemitted electrons and their flight time. The detector [7] combines an MCP and a P43 florescent screen which is imaged onto a PCO.2000 camera [11]. The MCP front–back potential difference (typically 1.25 kV) and the camera exposure time (typically 30 s) control the intensity of the recorded photoemission footprint.

Data were recorded for each photocathode under illumination with λ = (266 – 286) nm in intervals of 5 nm, then analysed according to our published methodology [9].

Surface Roughness Measurement

The surface roughness of the photocathodes was measured using a DME HS100M AFM with a DS 95-50 scanner and an ADE PhaseShift MicroXAM, each used to measure in 5 locations around the photocathode centre from where electrons are extracted. The AFM scans over 50 µm × 50 µm areas were repeated twice, and the MicroXAM scans using a 50× objective over 173 µm × 131 µm areas were repeated 4 times at each location. To increase surface coverage, the areas sampled by the AFM and optical techniques were not the same. The averaged results were as follows:

Table 1: Surface roughness measurements. TPH is the 10-point average height measurement (S_z), and RMS the root–mean square value with respect to the surface datum (S_q).

Sample	AFM [nm]		XAM [nm]	
	TPH	RMS	TPH	RMS
Cu.DT	728.6	83.4	919.7	81.9
Cu.EF	1083.2	143.9	1080.0	147.2
Mo	–	–	1691.6	241.4

The data in Table 1 show that the diamond–turned sample (Cu.DT) is smoother than the engineering finishes of both the copper (Cu.EF) and molybdenum photocathodes. The surface roughness of the Mo sample was so large that AFM measurement was not possible, so only optical data is shown.

EXPERIMENTAL RESULTS

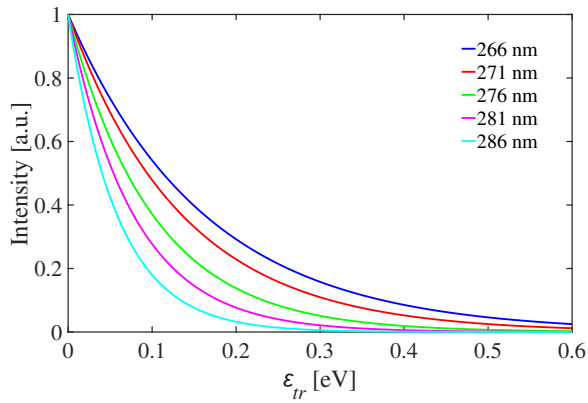

Figure 1: Fitted transverse energy spectra for the Cu.DT photocathode as a function of illumination wavelength. Similar spectra were obtained for the Cu.EF and Mo photocathodes.

Figure 1 shows the fitted transverse energy spectra (ε_{tr}) derived from measured data for the Cu.DT photocathode sample. Our MTE measurements as a function of illumination wavelength extracted from the ε_{tr} spectra at the $\frac{1}{e}$ level are summarised for all photocathode samples in Table 2.

Table 2: Summary of Measured MTE Values

Wavelength, λ [nm]	Sample, MTE [meV]		
	Cu.EF	Cu.DT	Mo
266	137.2	162.6	225.9
271	105.7	135.7	186.4
276	87.1	100.9	158.5
281	73.8	77.9	136.4
286	53.0	59.4	111.7

By plotting the MTE values shown in Table 2 and extrapolating the lines to the point MTE = kT equating to 25 meV at room temperature, we were able to extract an emission 'threshold wavelength' for each photocathode. This wavelength was then converted to an estimated workfunction for each photocathode sample studied. These plots are shown in Fig. 2, and a summary of both published and measured (extrapolated to kT) workfunctions are shown in Table 3.

The nature of our MTE measurements relies on the electron flight time τ which is driven by the drift distance d between the photocathode and the detector, and the accelerating field U_{acc} between them. The noise and ripple present in the voltages applied to the photocathode source and detector grid has a negligible effect on the extracted MTE, the dominant source of error being the drift distance between the source and detector. This has been measured to an accu-

ISBN 978-3-95450-182-3

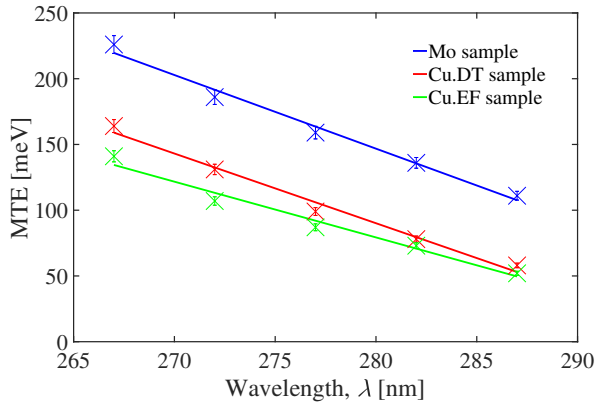

Figure 2: Extrapolation of MTEs to estimate the workfunction based on a photoemission threshold wavelength.

racy of ±1.4 % which equates to an error of ±3 % in our calculated ε_{tr} and MTE values once data is processed.

DISCUSSION

An increase in surface roughness leads to a decrease in the effective work function (ϕ_{eff}) due to the local electric field associated with such 'sharp' microstructure [4, 12, 13]. The effective work function is simply the difference between the normal workfunction (ϕ_0) and the Schottky voltage arising from the surface electric field. The voltages and corresponding electric fields (F) used in TESS experiments are very low compared to those typical of a photocathode electron gun (4 kV/m in TESS compared to 60 MV/m in an RF gun [3]), but this formalism is used for consistency with other published work. Thus an increase in surface roughness in turn causes the MTE to increase as the energy excess (ε) defined by the difference between the incident photon energy and the effective workfunction also increases:

$$\varepsilon = \frac{hc}{\lambda} - \phi_{eff} \quad \text{where} \quad \phi_{eff} = \phi_0 - \sqrt{\frac{e^3 F}{4\pi\varepsilon_0}} \qquad (1)$$

However our results do not exhibit this trend: the Cu.DT sample has lower surface roughness than the Cu.EF sample, and yet it exhibits higher MTE. Our data does show that the MTE for all of our photocathodes falls progressively as the illumination wavelength λ is increased, as predicted by equation (1). The tuning of illumination wavelength at accelerator facilities to minimise electron beam emittance in this way is technically feasible [1], albeit at the expense of photocathode QE.

We do not have an explanation for this behaviour at present, but will be carrying out a much more detailed set of MTE and work function measurements as a function of surface roughness in coming months.

The MTE values for Mo were recorded as being significantly higher than those for both Cu samples at all wavelengths, and this is driven by its very high surface roughness (see Table 1) and lower work function (see Table 3).

Table 3: Summary of published and measured work functions (ϕ_0) for polycrystalline copper and molybdenum.

Sample	Workfunction, ϕ_0 [eV]	
	Published	**Measured**
Cu.DT	4.65 [14]	4.26
Cu.EF		4.24
Mo	4.0 - 4.3 [15]	4.11

Workfunction can be a difficult physical property to measure, as evidenced by the variance in reported values in published data over many years. This is in part due to the nature of the measurements, the most common techniques being the use of either UPS or a Kelvin probe, which often deliver different results for the same surface. The precise nature of the surface also affects the workfunction, as different workfunctions are associated with different crystallographic faces. A polycrystalline surface is assumed to be a mixture of domains with various Miller indices, predominantly those with low–order values.

The extrapolated workfunction estimates shown in Table 3 are more accurate than those which might be obtained with a Kelvin probe as they are based on photoemission rather than comparison with a 'known' standard. The Kelvin probe may have the advantage of accessing workfunction information on a highly–localised sub–domain scale, however a measurement based on photoemission will inevitably sample a larger surface region, yielding a more pragmatic value which reflects an average surface workfunction as may be encountered when using a polycrystalline metal photocathode as a particle accelerator electron source.

CONCLUSIONS

Our results demonstrate that MTE is dependent on both surface roughness and work function, though we cannot distinguish the relative contribution of these quantities to the observed MTE.

The application of MTE measurements as a function of illumination wavelength provides a practical estimate of a surface work function.

FURTHER WORK

A more in–depth study is planned involving photocathodes of differing materials, with both single–crystal faces and polycrystalline samples prepared to the same known levels of surface roughness to investigate the effects of both work function and roughness on the MTE.

ACKNOWLEDGEMENTS

The authors gratefully acknowledge Mark Roper (STFC Daresbury Laboratory) for his help in our measurements of photocathode surface roughness.

The work is part of EuCARD-2, partly–funded by the European Commission under grant number GA 312453.

REFERENCES

[1] C.P. Hauri, R. Ganter *et al.*; PRL **104**, 234802 (2010).

[2] M.C. Divall, E. Prat, *et al.*; PRSTAB **18**, 033401 (2015).

[3] M. Krasilnikov; Proc. FEL '06, THPPH013, 583 – 586.

[4] W. Li and D.Y. Li; J. Chem. Phys **122**, 064708 (2005).

[5] D.H. Dowell, I.V. Bazarov *et al.*; NIM 'A' **622** (2010), 685 – 697.

[6] Z. Zhang and C. Tang; PRSTAB **18**, 053401 (2015).

[7] L.B. Jones, K.J. Middleman *et al.*; Proc. FEL '13, TUPS033, 290 – 293.

[8] S. Mistry, M. Cropper *et al.*; Proc. IPAC '16, THPMY017, 3691 – 3694.

[9] R. Beech, L.B. Jones *et al.*; Proc. IPAC '16, THPOW016, 3964–3967.

[10] https://www.pco.de/sensitive-cameras/pcoultraviolet/

[11] https://www.pco.de/camera-selector/pco2000/

[12] Y. Wan, Y. Li *et al.*; J. Elecrochem. Sci. **7**, 5204 – 5216 (2012).

[13] M. Xue, W. Wang *et al.*; J. Alloys Comp. **577** (2013) 1 – 5.

[14] O. Renault, R. Brochier *et al.*; Surf. Int. Anal. **38**, 375 (2006).

[15] R.G. Wilson; J. Appl. Phys. **37** (8), 3170 (1966).

ISBN 978-3-95450-182-3